Improved Plaque Assay Identifies a Novel Anti-*Chlamydia* Ceramide Derivative with Altered Intracellular Localization

Sebastian Banhart,[a] Essa M. Saied,[b,c] Andrea Martini,[a] Sophia Koch,[a] Lukas Aeberhard,[a,d] Kazimierz Madela,[e] Christoph Arenz,[b] Dagmar Heuer[a]

Junior Research Group "Sexually Transmitted Bacterial Pathogens" (NG 5), Robert Koch Institute, Berlin, Germany[a]; Organic and Bioorganic Chemistry, Department of Chemistry, Humboldt-Universität zu Berlin, Berlin, Germany[b]; Chemistry Department, Faculty of Science, Suez Canal University, Ismailia, Egypt[c]; Department of Molecular Biology, Max Planck Institute for Infection Biology, Berlin, Germany[d]; Advanced Light and Electron Microscopy (ZBS 4), Robert Koch Institute, Berlin, Germany[e]

***Chlamydia trachomatis* is a medically important human pathogen causing different diseases, including trachoma, the leading cause of preventable blindness in developing countries, and sexually transmitted infections that can lead to infertility and ectopic pregnancies. There is no vaccine against *C. trachomatis* at present. Broad-spectrum antibiotics are used as standard therapy to treat the infection but have unwanted side effects, such as inducing persistent or recurring infections and affecting the host microbiome, necessitating the development of novel anti-*Chlamydia* therapies. Here, we describe the establishment of a robust, fast, and simple plaque assay using liquid overlay medium (LOM) for the identification of anti-*Chlamydia* compounds. Using the LOM plaque assay, we identified nitrobenzoxadiazole (NBD)-labeled 1-*O*-methyl-ceramide-C_{16} as a compound that efficiently inhibits *C. trachomatis* replication without affecting the viability of the host cell. Further detailed analyses indicate that 1-*O*-methyl-NBD-ceramide-C_{16} acts outside the inclusion. Thereby, 1-*O*-methyl-NBD-ceramide-C_{16} represents a lead compound for the development of novel anti-*Chlamydia* drugs and furthermore constitutes an agent to illuminate sphingolipid trafficking pathways in *Chlamydia* infections.**

*C*hlamydia trachomatis* is an obligate intracellular human pathogen of high medical and socioeconomic importance (1). *C. trachomatis* can cause infections of the urogenital tract and trachoma, the leading cause of preventable blindness in developing countries. In women, untreated and recurring genital *C. trachomatis* infections can escalate, leading to severe sequelae, including pelvic inflammatory disease (PID), infertility, and ectopic pregnancies (2). Currently, no vaccine against *C. trachomatis* is available. For standard therapy, the Centers for Disease Control and Prevention (CDC) in the United States recommends either a single dose of 1 mg azithromycin or 100 mg doxycycline twice a day for at least 7 days for uncomplicated urogenital-tract *C. trachomatis* infections. These broad-spectrum antibiotics affect the normal microbial flora and can select for resistant strains or induce *Chlamydia* persistence (3–7). Like all members of the *Chlamydiales*, *C. trachomatis* has a unique cycle of development, characterized by the presence of two distinct bacterial forms (8). The infectious elementary body (EB) adheres to the host cell and triggers its invasion. After entering the cell, the bacteria are found inside a membrane-bound vacuole, the inclusion. EBs differentiate into metabolically active reticulate bodies (RBs), which divide by binary fission and redifferentiate into EBs at the end of the cycle. After release from the host cell, EBs can infect new mammalian cells, and the cycle starts again.

Chlamydia spp. are among the few bacteria that require sphingomyelin for growth, rendering this pathway a potential target for the development of specific anti-*Chlamydia* therapies (9). Sphingomyelin is synthesized by the transfer of a phosphocholine head group from phosphatidylcholine to ceramide (10). In uninfected cells, ceramide is transported from the endoplasmic reticulum to the Golgi apparatus via vesicles or by CERT, a ceramide transport protein (11). Sphingomyelin synthase 1 (SMS1) catalyzes the production of sphingomyelin at the trans-Golgi apparatus, and sphingomyelin is then found enriched in the plasma membrane and

membranes of the endosomal system (12). In *C. trachomatis*-infected HeLa cells, sphingomyelin accumulates in the bacteria (13–15). Sphingomyelin acquisition by *C. trachomatis* and *Chlamydia muridarum* depends on vesicular and nonvesicular transport processes (15–18). In *C. muridarum*-infected cells, bacterial sphingolipid uptake is partially blocked by brefeldin A and HPA-12 [*N*-(3-hydroxy-1-hydroxymethyl-3-phenylpropyl)dodecanamide], drugs that inhibit vesicular Arf1-dependent and nonvesicular CERT-dependent ceramide trafficking, respectively (17). Interestingly, HPA-12 but not brefeldin A treatment reduces the formation of infectious *C. muridarum* EBs (17).

Different means exist to analyze the *Chlamydia* cycle of development, including reinfection assays, electron microscopy, and real-time PCR. The gold standard to determine the effects of a specific treatment on progeny formation is titration of newly formed EBs by reinfection of fresh cells. Newly developed inclusions can then be counted directly by bright-field imaging or after immunostaining. Alternatively, EBs can also be titrated by plaque assay (19, 20). The current protocol for plaque titration of different *Chlamydia* strains uses a soft-agar overlay medium. This is a time-consuming method that is furthermore not easily transferred to a high-throughput screening format (19, 20).

Here, we describe a method for fast, robust, and easy titration

of *Chlamydia* spp. using a liquid overlay medium (LOM) plaque assay followed by immunodetection of formed plaques. Using this assay, we identified 1-*O*-methyl-ceramide-C_{16} labeled with the fluorophore nitrobenzoxadiazole (NBD) as a new anti-*Chlamydia* compound. In *C. trachomatis*-infected HeLa cells, 1-*O*-methyl-NBD-ceramide-C_{16} is not transported to the bacteria inside the inclusion and inhibits *C. trachomatis* EB formation. Thus, 1-*O*-methyl-NBD-ceramide-C_{16} constitutes a lead compound for the development of novel anti-*Chlamydia* drugs and furthermore represents a new agent to illuminate sphingolipid trafficking pathways in *Chlamydia* infections.

MATERIALS AND METHODS

Reagents and antibodies. Unless otherwise stated, all reagents were obtained from Sigma-Aldrich. Chloramphenicol (catalog no. 3886) was purchased from Carl Roth; the sphingomyelin synthase inhibitor D609 (catalog no. BML-ST330-0005) was obtained from Enzo Life Sciences. Ceramide compounds used in this study were NBD-ceramide-C_{16} and 1-*O*-methyl-NBD-ceramide-C_{16} (details on the chemical synthesis will be published elsewhere). All ceramide compounds were prepared as stock solutions containing 0.5 mM ceramide compound complexed to 0.5 mM defatted bovine serum albumin (BSA) and stored at $-20°C$ under desiccated conditions protected from light. The following antibodies were used in this study: mouse anti-Hsp60 (bacterial) (1:600; catalog no. ALX-804-072; Enzo Life Sciences), rabbit anti-IncA (1:500), rabbit anti-giantin (1:500; catalog no. PRB-114C; Covance), IRDye 680RD-coupled goat anti-mouse IgG (1:1,000; catalog no. 926-68070; Li-Cor Biosciences), Alexa Fluor 488-coupled goat anti-rabbit IgG (1:100; catalog no. 111-545-144; Dianova), Cy3-coupled goat anti-mouse IgG (1:200; catalog no. 115-165-146; Dianova), and Alexa Fluor 647-coupled goat anti-rabbit IgG (1:100; catalog no. 111-605-144; Dianova).

Polyclonal rabbit anti-IncA antibody was produced by immunization of rabbits with the C-terminal cytoplasmic fragment of IncA (N80–S246) fused to *Schistosoma japonicum* glutathione *S*-transferase (GST). All animal handling was performed by Biogenes, Berlin. The antigen was produced in *Escherichia coli* Rosetta 2 (Merck) using the pGEX-3X N-terminal GST expression vector (GE Healthcare). Cloning was done by using EcoRI and BamHI restriction sites in *E. coli* Top10 (Invitrogen). The primers used were 5′-CCCGGGGATCCATAATTTCATGCTGAGCG-3′ (forward) and 5′-CCCGGGAATTCCTAGGAGCTTTTTGTAGAGG-3′ (reverse). GST-IncA fusion protein was expressed and purified using Hi-Cap glutathione matrix slurry (Qiagen) according to the manufacturer's instructions. IncA-specific antibodies were affinity purified by depleting inactivated (56°C, 30 min) rabbit serum from GST-specific antibodies for 8 h, followed by binding to the cross-linked GST-IncA beads overnight. Beads were washed with 0.1 M borate, 0.5 M NaCl (pH 8.0) and eluted with 0.2 M glycine (pH 2.0) into 2 M Tris to neutralize the pH. Purified antibody was dialyzed against phosphate-buffered saline (PBS) and diluted 1:1 in glycerol, 0.06% (wt/vol) sodium azide for storage at $-20°C$.

Cell culture and infection. HeLa 229 cervical epithelial cells (ATCC CCL-2.1) and McCoy mouse fibroblasts (ATCC CRL-1696) were cultured in RPMI 1640 medium (Gibco) supplemented with 10% (vol/vol) heat-inactivated fetal calf serum (FCS; Biochrom), 1 mM sodium pyruvate, and 2 mM L-glutamine at 37°C and 5% (vol/vol) CO_2 in a humidified incubator. For time-lapse fluorescence microscopy, HeLa cells stably expressing *Aequorea victoria* green-fluorescent protein (GFP) were used. *C. trachomatis* lymphogranuloma venereum (LGV) biovar strain L2/434/Bu (ATCC VR-902B), *C. trachomatis* trachoma type A strain HAR-13 (ATCC VR-885), *C. trachomatis* trachoma type D strain UW-3/Cx (ATCC VR-571B), *C. psittaci* strain DC15, genotype A-VS1 (cattle isolate, 2002; kindly provided by Konrad Sachse, Institute of Molecular Pathogenesis, Friedrich-Loeffler-Institut, Jena, Germany), and *C. muridarum* mouse pneumonitis (MoPn) strain Nigg II (ATCC VR-123) were propagated in and purified from HeLa cell monolayers. Infections were performed in

Dulbecco's modified Eagle's medium (DMEM; Gibco) with glucose (4.5 g/liter) supplemented with 5% (vol/vol) fetal calf serum (FCS), 1 mM sodium pyruvate, and 2 mM L-glutamine (infection medium). Cells were washed twice with infection medium and incubated with bacteria using various multiplicities of infection (MOI) at 35°C and 5% (vol/vol) CO_2 in a humidified incubator. After 2 h, cells were again washed with infection medium and incubated at 35°C.

Agar-based plaque assay. For agar-based plaque assays, cells were seeded in multiwell plates for 70% confluence the next day. Cells were then incubated with dilutions of *Chlamydia* in infection medium for 2 h, followed by washing twice with infection medium. Subsequently, cells were overlaid with agar-containing medium according to Matsumoto et al. ([19]). Briefly, agar-based overlay medium was freshly prepared by mixing DMEM containing DEAE-dextran, $NaHCO_3$, and FCS with 2% (wt/vol) purified agar (L28) (LP0028B; Oxoid) preheated to 55°C (final concentrations: 0.01% [wt/vol] DEAE-dextran, 0.05% [wt/vol] $NaHCO_3$, 5% [vol/vol] FCS, 0.55% [wt/vol] agar). The mixture was immediately added to the cells and overlaid with infection medium after solidifying. Cells were incubated at 35°C for 8 days.

Liquid overlay medium-based plaque assay. For liquid overlay medium-based plaque assays, cells were seeded in 48-well plates (6- to 96-well plates were also successfully tested) for 70% confluence the next day. Cells were then incubated with dilutions of *Chlamydia* in 250 μl infection medium for 2 h, followed by washing twice with infection medium. Subsequently, cells were overlaid with 350 μl liquid overlay medium (DMEM containing 0.01% [wt/vol] DEAE-dextran, 0.05% [wt/vol] $NaHCO_3$, 5% [vol/vol] FCS, 0.6% [wt/vol] Avicel microcrystalline cellulose [RC-581; FMC BioPolymer]) following incubation at 35°C for 3 to 5 days. For inhibitor studies, liquid overlay medium was premixed with the respective compound and added at 8 h postinfection (p.i.) (see Fig. S1 in the supplemental material).

Plaque staining. For neutral red vital staining of agar-based plaques, infection medium was removed and agar was overlaid with neutral red staining solution (3% [wt/vol] neutral red in PBS, pH 7.4) and incubated for 4 h at 35°C. For crystal violet staining, infection medium was removed and the overlay was incubated with crystal violet staining solution (0.5% [wt/vol] crystal violet, 10% [wt/vol] formaldehyde in PBS, pH 7.4) overnight at room temperature. For immunofluorescence staining, cells were carefully washed three times with PBS to remove the overlay medium, fixed with 2% (wt/vol) formaldehyde in PBS for 30 min, and permeabilized with 0.2% (vol/vol) Triton X-100 in PBS for 15 min. Then, cells were stained for bacterial Hsp60 (secondary antibody: IRDye 680RD-coupled goat anti-mouse IgG; see "Immunofluorescence staining" below for experimental details). After a final wash with distilled H_2O, fluorescent signals were detected using an Odyssey infrared imaging system (model 9120; LiCor Biosciences).

Automated quantification of plaque numbers. For automated quantification of plaque numbers, image files of plaques were converted to grayscale using Photoshop CS6 software (Adobe) followed by image smoothing using the FIJI image processing package of the ImageJ software ([21]). Once smoothened, brightness levels were adjusted using the option "Threshold." Finally, particles were counted using the standard settings of the "Analyze Particles" function.

Reinfection assay. To determine the inhibitory effect of compounds on the formation of infectious progeny, cells were seeded in 6-well plates and infected with *C. trachomatis* L2 (MOI, 2). At 8 h p.i., compounds were added at a concentration of 4.65 μM (the 50% inhibitory concentration [IC_{50}] of 1-*O*-methyl-NBD-ceramide-C_{16}), and cells were harvested at various time points using a cell scraper. After glass bead lysis, lysates were titrated on freshly seeded HeLa 229 cells, fixed at 24 h p.i., and stained for Hsp60. Numbers of infection-forming units (IFU) per ml were calculated from average inclusion counts in 10 fields of view per condition.

Lactate dehydrogenase (LDH) cytotoxicity assay. For assessing the cytotoxic potential of the inhibitory compounds used in this study, an LDH cytotoxicity assay was performed according to the manufacturer's
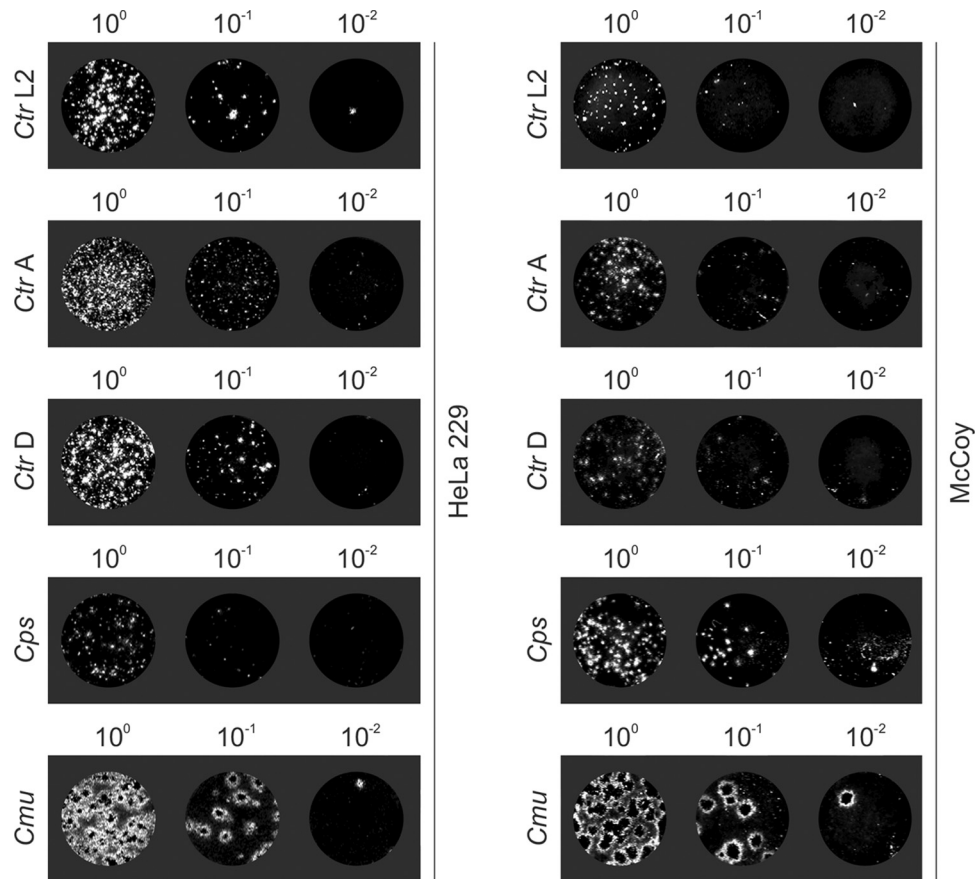
FIG 1 Novel plaque assay allows titration of *Chlamydia* species based on immunofluorescence staining. Immunofluorescence images show plaques of *C. trachomatis* L2 (*Ctr* L2), *C. trachomatis* A (*Ctr* A), *C. trachomatis* D (*Ctr* D), *C. psittaci* (*Cps*), and *C. muridarum* (*Cmu*) in a cell monolayer of HeLa 229 and McCoy cells. Cells were seeded in 48-well plates and infected with different titers. After 4 days of incubation, cells were fixed and stained for chlamydial Hsp60. Numbers indicate the dilution factor of the bacteria.

instructions (cytotoxicity detection kit PLUS; catalog no. 04 744 926 001; Roche Diagnostics). Briefly, cells were seeded in 96-well plates, infected with *C. trachomatis* L2 (MOI 2) or left uninfected, and incubated with the respective compounds at 8 h p.i. At 48 h p.i., cells were incubated with 100 µl of the supplied reaction mixture for 30 min at room temperature. The reaction was stopped by adding 50 µl of stop solution, followed by measuring absorbance at 492 nm using an Infinite 200 Pro plate reader (Tecan). Measured values were corrected for background and normalized to positive controls (cells lysed using the lysis reagent provided with the kit).

Ceramide uptake assay. To monitor intracellular distribution of ceramide compounds, *C. trachomatis* L2 (MOI, 2; 24 h p.i.)-infected and uninfected HeLa 229 cells were incubated with the respective ceramide compounds at a concentration of 25 µM at 35°C for 1 h, as previously described (22). Then, Hoechst 33342 (25 µg/ml) was added to stain for DNA, and confocal images were acquired using an LSM 780 laser scanning confocal microscope (Carl Zeiss).

Immunofluorescence staining. Samples were treated as previously published (23). Briefly, cells were washed with PBS, fixed with 2% (wt/vol) formaldehyde in PBS for 30 min at room temperature, and permeabilized with 0.2% (vol/vol) Triton X-100 and 0.2% (wt/vol) BSA in PBS for 15 min. Then, cells were incubated with primary antibodies diluted in 0.2% (wt/vol) BSA in PBS for 1 h at room temperature. After being washed with PBS, cells were incubated with secondary antibodies and the DNA stain 4′,6-diamidino-2-phenylindole (DAPI; 1:10,000) diluted in 0.2% (wt/vol) BSA in PBS for 1 h at room temperature and washed with PBS again.

Images were acquired using an LSM 780 laser scanning confocal microscope (Carl Zeiss).

Time-lapse fluorescence microscopy. HeLa cells stably expressing GFP were seeded in 35-mm imaging dishes (Ibidi), infected with a low dose of *C. trachomatis* L2, and overlaid with liquid overlay medium (see "Liquid overlay medium-based plaque assay" above for experimental details) at 2 h p.i. following incubation at 35°C. Fluorescence images were acquired every 15 min using an Eclipse TE2000-E widefield microscope (Nikon) with time-lapse imaging capability equipped with a Cascade 512B electron-multiplying charge-coupled device (EMCCD) camera (Photometrics).

Statistical analysis. Data are presented as means ± standard errors of the means. Significant differences between means were determined using Student's *t* test. *P* values below 0.05 were considered significant.

RESULTS

LOM plaque assay shows distinct plaque morphology of different *Chlamydia* spp. We first compared plaque formation in McCoy cells infected with *C. trachomatis* L2 at different MOIs under standard solid medium (Oxoid agar) and liquid overlay medium (LOM) by conventional crystal violet staining (see Fig. S2 in the supplemental material). Slightly larger plaques with clearer plaque morphology were detected under LOM conditions than with standard solid overlay medium. Additionally, the LOM plaque assay allowed the specific detection of *C. trachomatis* plaques by anti-
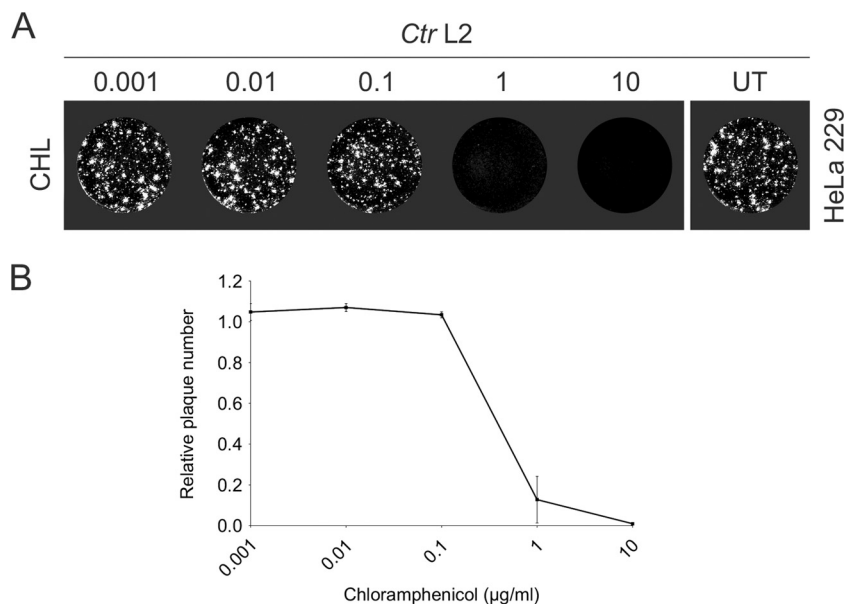
FIG 2 Inhibitory compounds can be screened and quantified for their anti-*Chlamydia* activity. (A) Immunofluorescence images showing *C. trachomatis* L2 (*Ctr* L2) plaques in a HeLa 229 cell monolayer after incubation with different concentrations of chloramphenicol. Cells were seeded in 48-well plates, infected with *C. trachomatis* L2 (MOI, 0.003; approximately 300 IFU per well), and, at 8 h p.i., incubated with chloramphenicol (CHL; concentrations are in µg/ml). After 4 days of incubation, cells were fixed and stained for chlamydial Hsp60. UT, untreated controls. (B) Quantification of relative plaque numbers. Plaque numbers were normalized to untreated controls ($n = 2$; error bars indicate standard errors [SE]).

Chlamydia Hsp60 immunostaining (see Fig. S2 in the supplemental material). Next, plaque formation of different *Chlamydia* spp. in HeLa 229 and McCoy cells under LOM plaque assay conditions was assessed (Fig. 1). All *Chlamydia* strains tested, including *C. trachomatis* L2, *C. trachomatis* A and D, *C. psittaci*, and *C. muridarum*, formed detectable plaques in an MOI-dependent manner in the two different cell lines after 4 days p.i. Interestingly, the morphology of *C. muridarum* plaques differed from the plaque morphology of *C. trachomatis* and *C. psittaci*. In *C. muridarum* infections, plaques were larger and showed a rim-like Hsp60 staining pattern indicative of cytotoxicity, known to be associated with *C. muridarum* (24). Moreover, clonal variations of *Chlamydia* infections can be assessed on a subcellular level (see Fig. S3 in the supplemental material). In sum, the LOM plaque assay is a fast, robust, and antigen-specific titration method for different *Chlamydia* spp. in various cell lines and allows the discrimination of *Chlamydia* spp. by plaque morphology.

LOM plaque numbers of *C. trachomatis* were reduced after chloramphenicol treatment. We tested if our established LOM plaque assay would allow the identification of anti-*Chlamydia* compounds by addition of chloramphenicol, an antibiotic that inhibits bacterial protein synthesis (Fig. 2A). Cells were infected with *C. trachomatis* L2, and at 8 h p.i., different concentrations of chloramphenicol were added to the cell layer together with the overlay medium. Plaques were visualized 4 days p.i. by immunofluorescence and counted using ImageJ. Clear and distinct *C. trachomatis* plaques were detected for concentrations below 1 µg/ml (1.09 µM) chloramphenicol. At 1 µg/ml chloramphenicol the formation of *C. trachomatis* plaques was completely blocked (Fig. 2A). Based on the data obtained, we determined the IC$_{50}$ of chloramphenicol by plotting the concentrations of chloramphenicol against relative plaque numbers, yielding an IC$_{50}$ of 2.77 µM (0.90 µM/ml) (Fig. 2B; Table 1). This demonstrates that anti-*Chlamydia*

compounds can be identified by and IC$_{50}$s can be calculated from LOM plaque assays.

1-*O*-Methyl-NBD-ceramide-C$_{16}$ acts as a novel anti-*Chlamydia* compound. *Chlamydia* spp. are auxotrophic for different nutrients, including sphingolipids (9, 25). Recent data showed an effect of the sphingomyelin synthase inhibitor D609 on uptake of fluorescently labeled ceramide by *C. muridarum*; however, the effect of the inhibitor on bacterial propagation was not addressed (17). D609 acts on different enzymes of the eukaryotic host cell, including SMS1, SMS2, and the phosphatidylcholine-specific phospholipase C (PLC) (26). To test the effect of SMS inhibition by D609 on *C. trachomatis* propagation, a LOM plaque assay was performed in the presence of D609 at various concentrations. A clear reduction in plaque numbers was observed at a concentration of 25 µg/ml (93.82 µM/ml) D609, demonstrating that inhibition of D609-sensitive pathways efficiently impedes chlamydial propagation (Fig. 3A). To understand the impact of SM production on *C. trachomatis* propagation, we synthesized ceramide-C$_{16}$ derivatives labeled with NBD, NBD-ceramide-C$_{16}$, and 1-*O*-methyl-NBD-ceramide-C$_{16}$ (Fig. 3B) and analyzed their impact on *C. trachomatis* propagation by LOM plaque assay (Fig. 3C).

TABLE 1 IC$_{50}$s of inhibitory compounds used in this study[a]

Compound	IC$_{50}$ (µg/ml)		IC$_{50}$ (µM)	
	Mean	SE	Mean	SE
Chloramphenicol	0.90	0.46	2.77	1.43
D609	20.91	0.79	78.47	2.97
1-*O*-Methyl-NBD-ceramide-C$_{16}$	3.13	0.45	4.65	0.67

[a] Values were calculated on the basis of a sigmoidal dose-response curve with Prism 5 (GraphPad) using relative plaque numbers given in Fig. 2 and 3 ($n = 2$ for CHL and D609; $n = 4$ for 1-*O*-methyl-NBD-ceramide-C$_{16}$).
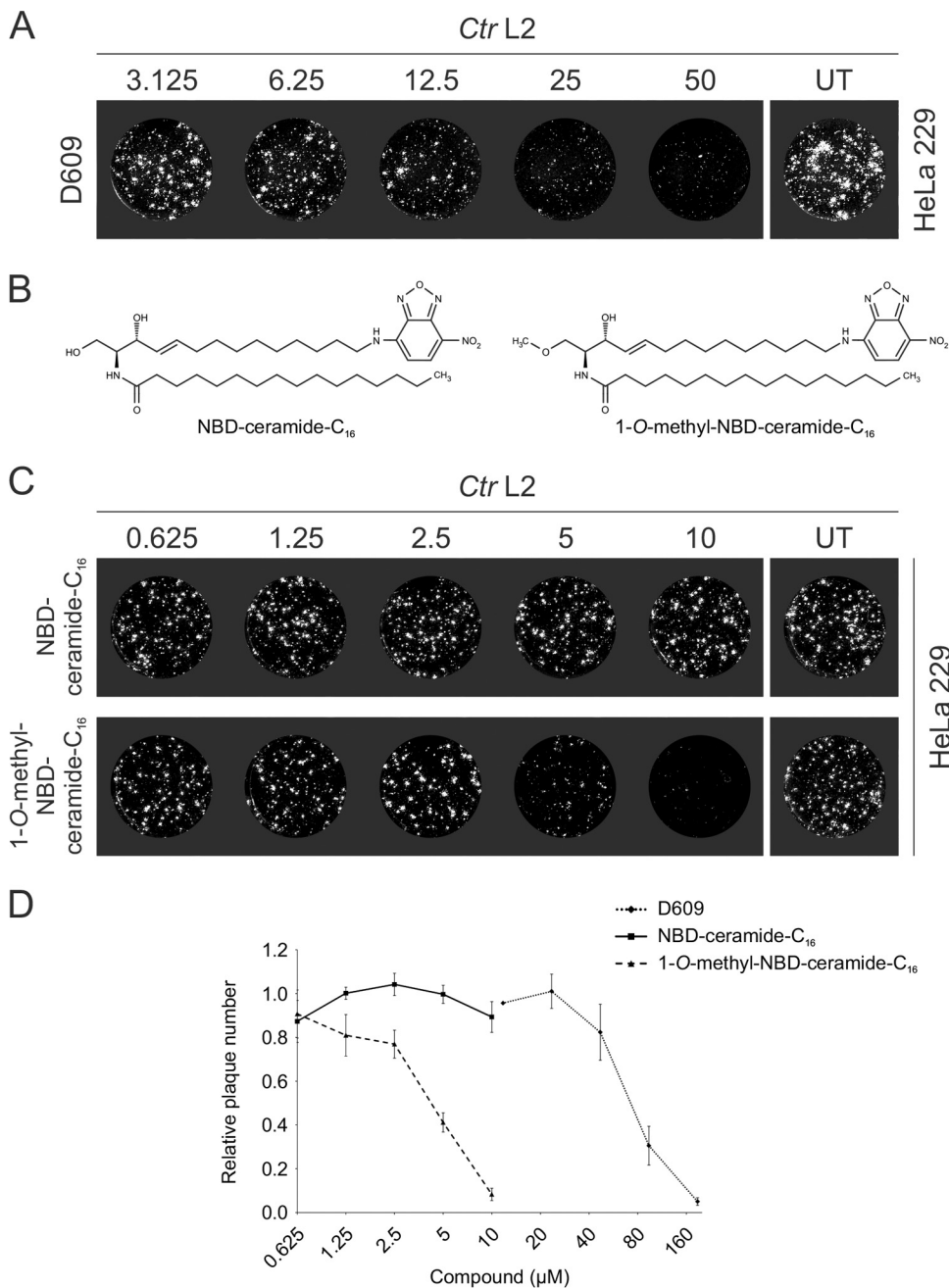
FIG 3 1-*O*-Methyl-NBD-ceramide-C_{16} inhibits plaque formation of *C. trachomatis* L2. (A) Immunofluorescence images showing *C. trachomatis* L2 (*Ctr* L2) plaques in a HeLa 229 cell monolayer after incubation with different concentrations of D609. Cells were seeded in 48-well plates, infected with *C. trachomatis* L2 (MOI 0.003; approximately 300 IFU per well), and, at 8 h p.i., incubated with D609 (μg/ml). After 4 days of incubation, cells were fixed and stained for chlamydial Hsp60. UT, untreated controls. (B) Chemical structures of NBD-ceramide-C_{16} and 1-*O*-methyl-NBD-ceramide-C_{16}. (C) Immunofluorescence images showing *C. trachomatis* L2 (*Ctr* L2) plaques in a HeLa 229 cell monolayer after incubation with different concentrations of anti-*Chlamydia* compounds. Cells were seeded in 48-well plates, infected with *C. trachomatis* L2 (MOI, 0.003; approximately 300 IFU per well), and, at 8 h p.i., incubated with NBD-ceramide-C_{16} and 1-*O*-methyl-NBD-ceramide-C_{16} (concentrations are in μM units). After 4 days of incubation, cells were fixed and stained for chlamydial Hsp60. (D) Quantification of relative plaque numbers. Plaque numbers were normalized to those of untreated controls ($n = 2$ for D609; $n = 4$ for ceramide compounds; error bars indicate SE).

1-*O*-Methyl-NBD-ceramide-C_{16} is a derivative of NBD-ceramide-C_{16} and resembles to a large extent a compound called 1-*O*-methyl-C_6-NBD-ceramide. The latter was previously shown not to be converted to sphingomyelin and to be transported to the Golgi apparatus by lower kinetics than NBD-ceramide-C_6 (27). 1-*O*-methyl-NBD-ceramide-C_{16} treatment clearly reduced plaque numbers at 5 μM (3.37 μg/ml) compared to infected cells treated with the identical concentration of NBD-ceramide-C_{16} (Fig. 3C and D). We next compared the IC_{50} of 1-*O*-methyl-NBD-ceramide-C_{16} with those of chloramphenicol and D609 (Table 1).
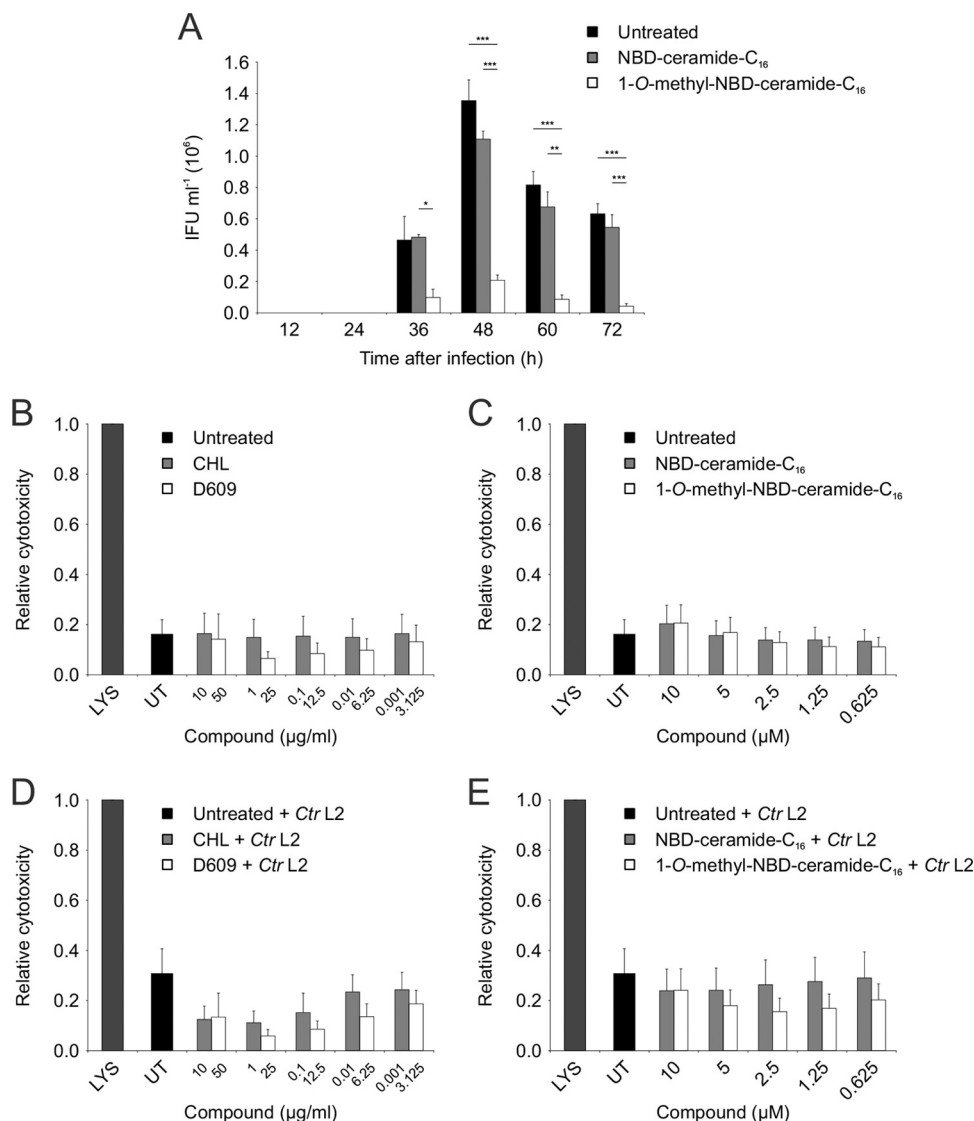
FIG 4 1-*O*-Methyl-NBD-ceramide-C$_{16}$ reduces *C. trachomatis* progeny formation but has no impact on cell viability. (A) Graph showing chlamydial replication at the indicated time points after incubation without (untreated) or with ceramide compounds. Cells were seeded in 6-well plates and infected with *C. trachomatis* L2 (MOI 2), and, at 8 h p.i., ceramide compounds were added at a concentration of 4.65 μM (the IC$_{50}$ of 1-*O*-methyl-NBD-ceramide-C$_{16}$). Cells were harvested at the indicated time points, titrated on freshly seeded cells, fixed at 24 h p.i., and stained for Hsp60. Chlamydial replication is expressed as infection-forming units (IFU) per ml (*n* = 3; error bars indicate SE). (B to E) Relative cytotoxicity of compounds used in this study for uninfected (B and C) and infected (D and E) cells, as measured by LDH release. Cells were seeded in 96-well plates, infected with *C. trachomatis* L2 (*Ctr* L2; MOI, 2) or left uninfected, and, at 8 h p.i., incubated with different concentrations of chloramphenicol (CHL; concentrations are in μg/ml), D609 (concentrations are in μg/ml), NBD-ceramide-C$_{16}$ (concentrations are in μM units), and 1-*O*-methyl-NBD-ceramide-C$_{16}$ (concentrations are in μM units). After 2 days of incubation, LDH release was measured using a spectrophotometric microplate reader. Values are corrected for background and normalized to positive control (lysed cells) (*n* = 2 for CHL and D609; *n* = 3 for ceramide compounds; error bars indicate SE).

The IC$_{50}$ of 1-*O*-methyl-NBD-ceramide-C$_{16}$ (4.65 μM [3.13 μg/ml]) was in the range of that of chloramphenicol (IC$_{50}$ of 2.77 μM [0.90 μg/ml]), and interestingly, 1-*O*-methyl-NBD-ceramide-C$_{16}$ was 17 times more effective than D609 (IC$_{50}$ of 78.47 μM [20.91 μg/ml]), showing that 1-*O*-methyl-NBD-ceramide-C$_{16}$ is a very potent and novel anti-*Chlamydia* compound.

1-*O*-Methyl-NBD-ceramide-C$_{16}$ reduces *C. trachomatis* EB formation but not cell viability. We next assessed the effect of 1-*O*-methyl-NBD-ceramide-C$_{16}$ on the production of infectious *C. trachomatis* EBs during the cycle of development. Infected HeLa cells were treated with 4.65 μM (the IC$_{50}$ of 1-*O*-methyl-

NBD-ceramide-C$_{16}$) NBD-labeled ceramides or left untreated. At various time points, cells were lysed, and EBs were titrated. A reduction in infectious EBs up to one order of magnitude was observed after treatment with a single dose of 1-*O*-methyl-NBD-ceramide-C$_{16}$ (Fig. 4A). The treatment did not affect the progression of the developmental cycle, as production of infectious EBs peaked at 2 days p.i. for treated as well as untreated conditions (Fig. 4A), indicating that the compound directly targets either bacterial growth or the production of infectious EBs. To further exclude effects on host cell viability, an LDH cytotoxicity assay of infected and uninfected cells after treatment with the different
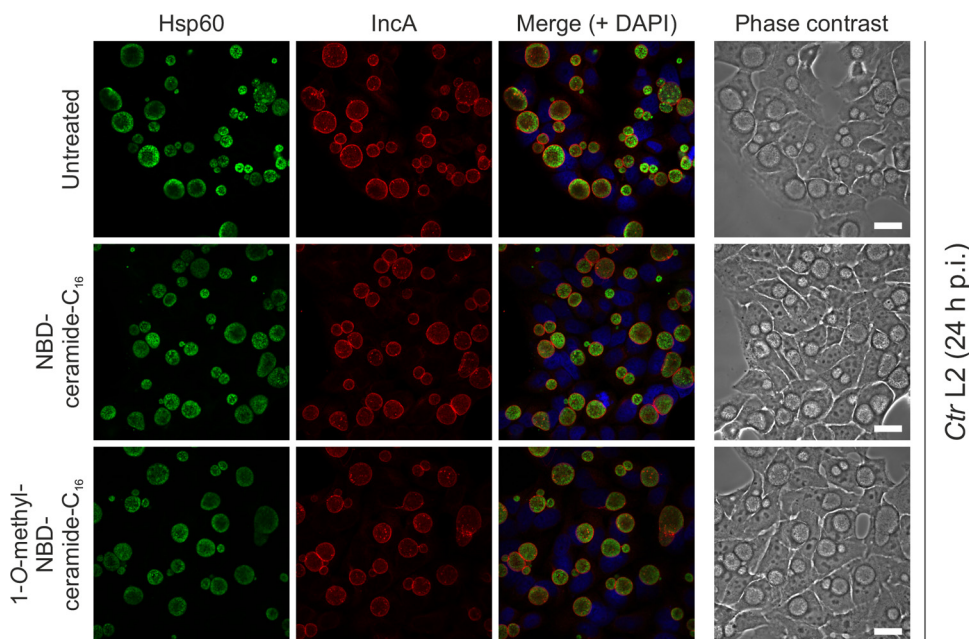
FIG 5 Inclusion formation is not affected by 1-*O*-methyl-NBD-ceramide-C_{16}. Immunofluorescence images show bacterial Hsp60 and IncA in *C. trachomatis* L2 (*Ctr* L2; MOI, 2) infected and noninfected (NI) HeLa 229 cells upon treatment with ceramide compounds. At 8 h p.i., ceramide compounds were added at a concentration of 4.65 μM (the IC_{50} of 1-*O*-methyl-NBD-ceramide-C_{16}). Cells were fixed at 24 h p.i. and stained with antibodies against chlamydial Hsp60 (green) and IncA (red); DNA was stained with DAPI (blue). Scale bar, 20 μm. Images are representative of three independent experiments.

compounds was performed (Fig. 4B to E). In uninfected cells, no signs of cytotoxicity were observed after treatment (Fig. 4B and C). Upon infection, untreated cells showed a marginal increase in cytotoxicity that was due to the infection. Thus, treatment with the inhibitory compound even slightly decreased *C. trachomatis*-dependent cytotoxicity (Fig. 4D and E). In sum, our compound strongly reduces the formation of infectious *C. trachomatis* EBs at a concentration that does not affect host cell viability.

1-*O*-Methyl-NBD-ceramide-C_{16} does not affect inclusion formation. Our data suggest that 1-*O*-methyl-NBD-ceramide-C_{16} interferes either with bacterial growth or with the formation of infectious EBs. To differentiate between these two possibilities, we analyzed the size and appearance of *C. trachomatis* inclusions in untreated, control-treated, and 1-*O*-methyl-NBD-ceramide-C_{16}-treated HeLa cells by immunofluorescence microscopy (Fig. 5). At 24 h p.i. cells were fixed, stained for the bacterial antigens Hsp60 and IncA, and visualized with a laser scanning confocal microscope. No significant differences in inclusion formation, appearance, or size were detected after 1-*O*-methyl-NBD-ceramide-C_{16} treatment compared to controls at 24 h p.i. (Fig. 5), demonstrating that 1-*O*-methyl-NBD-ceramide-C_{16} does not affect inclusion formation and suggesting that bacterial growth is not affected.

1-*O*-Methyl-NBD-ceramide-C_{16} is not taken up by *C. trachomatis*. To further understand the mode of action of the new compound, we analyzed the cellular localization of NBD-ceramide-C_{16} and 1-*O*-methyl-NBD-ceramide-C_{16} in *C. trachomatis*-infected and uninfected HeLa cells by live-cell microscopy. After 60 min of incubation, NBD-ceramide-C_{16} was incorporated into the bacteria inside the inclusion (Fig. 6). In contrast, the inhibitory compound 1-*O*-methyl-NBD-ceramide-C_{16} did not accumulate inside *C. trachomatis* inclusions but rather showed cytoplasmic fluorescence and a slight staining of the Golgi apparatus

(Fig. 6), demonstrating that only NBD-ceramide-C_{16} but not 1-*O*-methyl-NBD-ceramide-C_{16} was incorporated into the bacteria. This suggests that 1-*O*-methyl-NBD-ceramide-C_{16} operates outside the bacteria targeting either a host cell factor or a secreted bacterial protein and may indicate that sphingolipid transport across the inclusion membrane to the bacteria requires metabolism.

DISCUSSION

We have established a fast and robust plaque assay for the identification of new anti-*Chlamydia* compounds based on a previously published plaque assay to assess viral replication (28). Using this liquid overlay medium (LOM)-based plaque assay, we found that a single dose of 1-*O*-methyl-NBD-ceramide-C_{16} strongly reduces the number of infectious EBs. In contrast to NBD-ceramide-C_{16}, 1-*O*-methyl-NBD-ceramide-C_{16} did not accumulate in the bacteria inside the inclusion, suggesting that this compound acts on factors outside the bacteria.

Plaque formation assays are useful tools for the titration of different microorganisms and allow the identification of new antimicrobial substances, as they cover all stages of an infection process by capturing multiple rounds of infections. For many microorganisms, a solid overlay medium is necessary to prevent movement and spread of the organisms. For *Chlamydia*, plaque assays have been developed that use an agarose-based overlay medium (19, 20, 29). Although agarose concentrations had already been reduced to 0.5%, keeping cells in a good state, even the fast-growing strains *C. trachomatis* D and L2 needed 13 days to form detectable plaques under these conditions (19). In contrast, the established LOM plaque procedure reduces the required time for detection of plaques from different *Chlamydia* spp., including the slow-growing trachoma biovar *C. trachomatis* A, to less than 5
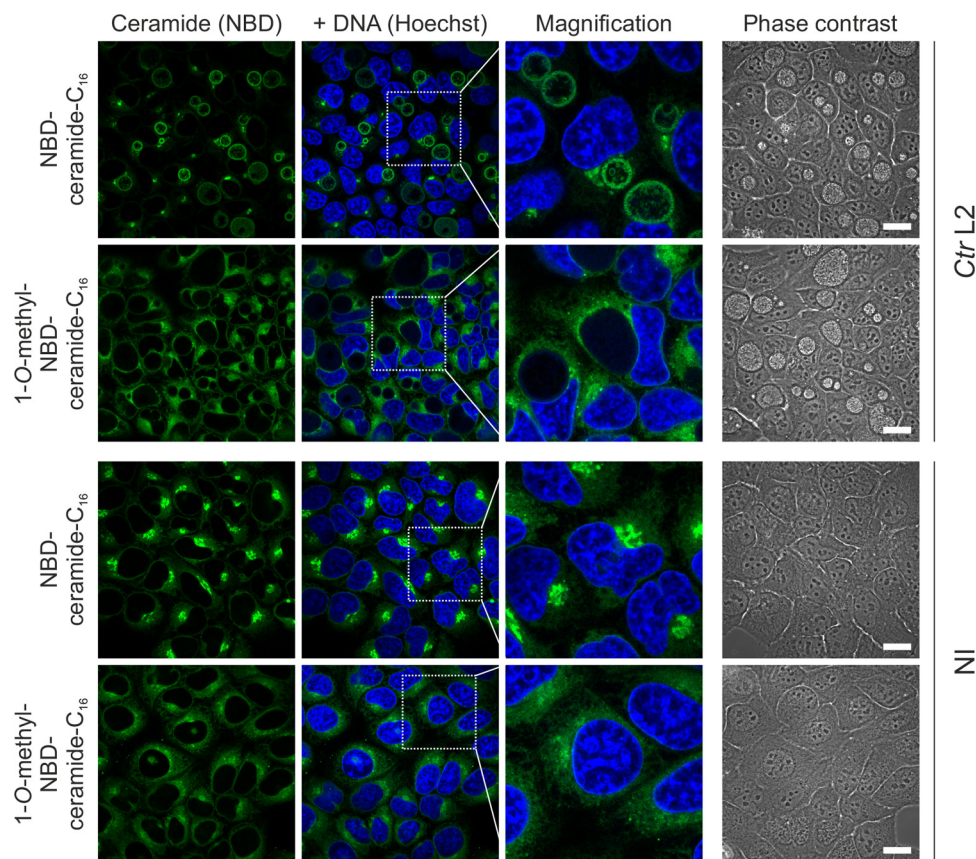
FIG 6 1-*O*-Methyl-NBD-ceramide-C_{16} is not translocated into the chlamydial inclusion. Fluorescence images show the localization of NBD-labeled ceramide compounds in *C. trachomatis* L2 (*Ctr* L2; MOI, 2)-infected and noninfected (NI) HeLa 229 cells. At 24 h p.i., ceramide compounds were added at a concentration of 25 μM. After incubation for 1 h at 35°C, DNA was stained with Hoechst 33342, and images were acquired using laser scanning confocal microscopy. Scale bar, 20 μm. Images are representative of three independent experiments.

days. Thus, the LOM plaque assay is nearly three times faster than the standard *Chlamydia* plaque assay. Compared to titration of infectious EBs by reinfection assays, the LOM plaque assay is less labor-intensive and can easily be adapted to a 96-well-plate format to screen for novel anti-*Chlamydia* compounds. Another advantage of the established assay is the use of *Chlamydia*-specific antibodies for detection of plaques. Immunodetection increases sensitivity and specificity of the described assay compared to a classical visualization of plaques by crystal violet staining. In addition, different *Chlamydia* species and the expression of different proteins can be distinguished based on plaque morphology and by using different protein-specific antibodies, respectively. Thus, the LOM plaque assay can visualize differences between clonal variants and phase variations at the subcellular level, which will help to further describe and understand *Chlamydia* diversity.

Chloramphenicol is often used in *Chlamydia* research to analyze the contribution of bacterial proteins to a specific process by blocking chlamydial protein synthesis. It affects the growth of the *Chlamydia* inclusion at concentrations higher than 0.4 μg/ml (30). These observations are in good agreement with our LOM plaque titration, which showed reduced plaque formation starting at concentrations higher than 0.1 μg/ml (1.09 μM) chloramphenicol, demonstrating the reliability and usability of our assay to identify anti-*Chlamydia* compounds.

The intricate interaction of *Chlamydia* with its host cell and its dependency on scavenging host sphingolipids constitute a possible Achilles' heel that can be exploited for the development of novel anti-*Chlamydia* compounds. To test this hypothesis, we treated *C. trachomatis*-infected HeLa cells with D609, a known SMS inhibitor. D609 treatment dramatically reduced plaque formation, confirming the importance of sphingomyelin for *C. trachomatis* infection. D609 is a drug that targets cellular sphingolipid synthases but, in addition, has pleiotropic effects on the host cell, including Zn^{2+} chelation, increased metabolic activity, and decreased ROS formation (26). To limit these unwanted side effects, we hypothesized that a ceramide analogue that cannot be converted to sphingomyelin would inhibit bacterial propagation more efficiently and more specifically. Therefore, an analogue was synthesized by methylation of the 1-hydroxy group. One dose of 1-*O*-methyl-NBD-ceramide-C_{16} (4.65 μM [3.13 μg/ml]) decreased the number of infectious EBs by more than one order of magnitude without any obvious effects on cell viability, as measured by LDH release, rendering this compound a potential new lead substance for the development of novel anti-*Chlamydia* drugs. Interestingly, *Toxoplasma gondii* and *Salmonella enterica* have also been shown to scavenge cellular sphingolipid pathways, and orthologs of the human SMS have been identified in the genome of *Plasmodium falciparum* (31–33). It will be interesting to analyze the inhibitory effect of 1-*O*-methyl-NBD-ceramide-C_{16}

on these additional medically important, intracellular human pathogens.

Although we currently do not understand how 1-*O*-methyl-NBD-ceramide-C$_{16}$ operates on *C. trachomatis*, it is likely that a cellular protein, possibly CERT, is targeted by this compound. This view is supported by the analysis of trafficking of fluorescently labeled ceramide compounds using live-cell microcopy. *Chlamydia* spp. incorporate fluorescently labeled ceramides with short fatty acid chains, as documented by different groups (13–15, 17). These derivatives are commonly used in cell biology to analyze sphingolipid trafficking; however, naturally occurring ceramides have longer acyl chains which give rise to differences in their polarity and transport routes (27). We therefore used NBD-ceramide-C$_{16}$ to analyze the trafficking of a ceramide with a native acyl chain length in *C. trachomatis*-infected HeLa cells and showed that ceramides with natural fatty acids also accumulate inside the bacteria within the inclusion. Surprisingly, 1-*O*-methyl-NBD-ceramide-C$_{16}$ was not transported to *C. trachomatis* but remained in the cytoplasm of the infected host cell outside the inclusion. This suggests that 1-*O*-methyl-NBD-ceramide-C$_{16}$ binds to a protein with higher affinity than NBD-ceramide-C$_{16}$. Alternatively, transport of sphingomyelin across the inclusion membrane is either dependent on the phosphocholine head group or directly coupled to SM synthesis. The latter view is supported by the observations of Elwell et al. (17) showing that human SMS2 is recruited to the *C. muridarum* inclusion membrane. Further studies are on the way to understand the mode of action of 1-*O*-methyl-NBD-ceramide-C$_{16}$.

Beside its anti-chlamydial activity, 1-*O*-methyl-NBD-ceramide-C$_{16}$ might become a useful tool to understand sphingolipid metabolism and transport in infected cells. It is known that C$_6$-NBD ceramide, labeled within its fatty acid part, is almost exclusively localized to the Golgi apparatus in uninfected cells (34). Schwarzmann et al. showed that the same holds true for the 3-*O*-methyl ether but not for the 1-*O*-methyl ether of C$_6$-NBD-ceramide, which cannot be converted to sphingomyelin or glycosphingolipids, suggesting that metabolism of ceramide is required for Golgi staining (27). It is noteworthy that the 1-*O*-methyl ether of ceramide not only differs from the previously reported compound by fatty acid chain length but also is the NBD dye attached to the sphingosine part of ceramide and not to the fatty acid part. However, the special feature of this novel ceramide derivative is that it is not further converted to sphingomyelin or glycosphingolipids. The observation that this compound does not accumulate inside the inclusion suggests that only sphingomyelin is taken up by *C. trachomatis*, confirming previously published biochemical data for isolated EBs (35).

We have shown that our established LOM plaque assay is a useful technique to rapidly and robustly analyze effects of different compounds on *Chlamydia* propagation and have identified 1-*O*-methyl-NBD-ceramide-C$_{16}$ as a novel anti-*Chlamydia* lead compound that can be used to better understand sphingolipid transport to and across the bacterial inclusion membrane.

ACKNOWLEDGMENTS

REFERENCES

1. Balabanova Y, Gilsdorf A, Buda S, Burger R, Eckmanns T, Gärtner B, Gross U, Haas W, Hamouda O, Hübner J, Jänisch Kist TM, Kramer MH, Ledig T, Mielke M, Pulz M, Stark K, Suttorp N, Ulbrich U, Wichmann O, Krause G. 2011. Communicable diseases prioritized for surveillance and epidemiological research: results of a standardized prioritization procedure in Germany, 2011. PLoS One 6:e25691. http://dx.doi.org/10.1371/journal.pone.0025691.

2. Haggerty CL, Gottlieb SL, Taylor BD, Low N, Xu F, Ness RB. 2010. Risk of sequelae after Chlamydia trachomatis genital infection in women. J. Infect. Dis. 201(Suppl):S134–S155. http://dx.doi.org/10.1086/652395.

3. Sweet RL, Schachter J, Robbie MO. 1983. Failure of beta-lactam antibiotics to eradicate Chlamydia trachomatis in the endometrium despite apparent clinical cure of acute salpingitis. JAMA 250:2641–2645. http://dx.doi.org/10.1001/jama.1983.03340190043029.

4. Augenbraun M, Bachmann L, Wallace T, Dubouchet L, McCormack W, Hook EW. 1998. Compliance with doxycycline therapy in sexually transmitted diseases clinics. Sex. Transm. Dis. 25:1–4. http://dx.doi.org/10.1097/00007435-199801000-00001.

5. Dean D, Suchland RJ, Stamm WE. 2000. Evidence for long-term cervical persistence of Chlamydia trachomatis by omp1 genotyping. J. Infect. Dis. 182:909–916. http://dx.doi.org/10.1086/315778.

6. Hogan RJ, Mathews SA, Mukhopadhyay S, Summersgill JT, Timms P. 2004. Chlamydial persistence: beyond the biphasic paradigm. Infect. Immun. 72:1843–1855. http://dx.doi.org/10.1128/IAI.72.4.1843-1855.2004.

7. Bhengraj AR, Vardhan H, Srivastava P, Salhan S, Mittal A. 2010. Decreased susceptibility to azithromycin and doxycycline in clinical isolates of Chlamydia trachomatis obtained from recurrently infected female patients in India. Chemotherapy 56:371–377. http://dx.doi.org/10.1159/000314998.

8. Bastidas RJ, Elwell CA, Engel JN, Valdivia RH. 2013. Chlamydial intracellular survival strategies. Cold Spring Harb. Perspect. Med. 3:a010256. http://dx.doi.org/10.1101/cshperspect.a010256.

9. van Ooij C, Kalman L, Van Ijzendoorn S, Nishijima M, Hanada K, Mostov K, Engel JN. 2000. Host cell-derived sphingolipids are required for the intracellular growth of Chlamydia trachomatis. Cell. Microbiol. 2:627–637. http://dx.doi.org/10.1046/j.1462-5822.2000.00077.x.

10. Ullman MD, Radin NS. 1974. The enzymatic formation of sphingomyelin from ceramide and lecithin in mouse liver. J. Biol. Chem. 249:1506–1512.

11. Hanada K, Kumagai K, Yasuda S, Miura Y, Kawano M, Fukasawa M, Nishijima M. 2003. Molecular machinery for non-vesicular trafficking of ceramide. Nature 426:803–809. http://dx.doi.org/10.1038/nature02188.

12. Hullin-Matsuda F, Taguchi T, Greimel P, Kobayashi T. 2014. Lipid compartmentalization in the endosome system. Semin. Cell Dev. Biol. 31C:48–56. http://dx.doi.org/10.1016/j.semcdb.2014.04.010.

13. Hackstadt T, Rockey DD, Heinzen RA, Scidmore MA. 1996. Chlamydia trachomatis interrupts an exocytic pathway to acquire endogenously synthesized sphingomyelin in transit from the Golgi apparatus to the plasma membrane. EMBO J. 15:964–977.

14. Scidmore MA, Fischer ER, Hackstadt T. 2003. Restricted fusion of Chlamydia trachomatis vesicles with endocytic compartments during the initial stages of infection. Infect. Immun. 71:973–984. http://dx.doi.org/10.1128/IAI.71.2.973-984.2003.

15. Heuer D, Rejman Lipinski A, Machuy N, Karlas A, Wehrens A, Siedler F, Brinkmann V, Meyer TF. 2009. Chlamydia causes fragmentation of the Golgi compartment to ensure reproduction. Nature 457:731–735. http://dx.doi.org/10.1038/nature07578.

16. Rejman Lipinski A, Heymann J, Meissner C, Karlas A, Brinkmann V, Meyer TF, Heuer D. 2009. Rab6 and Rab11 regulate Chlamydia trachomatis development and golgin-84-dependent Golgi fragmentation. PLoS Pathog. 5:e1000615. http://dx.doi.org/10.1371/journal.ppat.1000615.

17. Elwell CA, Jiang S, Kim JH, Lee A, Wittmann T, Hanada K, Melancon

P, Engel JN. 2011. Chlamydia trachomatis co-opts gbf1 and cert to acquire host sphingomyelin for distinct roles during intracellular development. PLoS Pathog. 7:e1002198. http://dx.doi.org/10.1371/journal.ppat.1002198.

18. Derre I, Swiss R, Agaisse H. 2011. The lipid transfer protein CERT interacts with the Chlamydia inclusion protein IncD and participates to ER-Chlamydia inclusion membrane contact sites. PLoS Pathog. 7:e1002092. http://dx.doi.org/10.1371/journal.ppat.1002092.

19. Matsumoto A, Izutsu H, Miyashita N, Ohuchi M. 1998. Plaque formation by and plaque cloning of Chlamydia trachomatis biovar trachoma. J. Clin. Microbiol. 36:3013–3019.

20. Gieffers J, Belland RJ, Whitmire W, Ouellette S, Crane D, Maass M, Byrne GI, Caldwell HD. 2002. Isolation of Chlamydia pneumoniae clonal variants by a focus-forming assay. Infect. Immun. 70:5827–5834. http://dx.doi.org/10.1128/IAI.70.10.5827-5834.2002.

21. Schindelin J, Arganda-Carreras I, Frise E, Kaynig V, Longair M, Pietzsch T, Preibisch S, Rueden C, Saalfeld S, Schmid B, Tinevez J-Y, White DJ, Hartenstein V, Eliceiri K, Tomancak P, Cardona A. 2012. Fiji: an open-source platform for biological-image analysis. Nat. Methods 9:676–682. http://dx.doi.org/10.1038/nmeth.2019.

22. Bhabak KP, Hauser A, Redmer S, Banhart S, Heuer D, Arenz C. 2013. Development of a novel FRET probe for the real-time determination of ceramidase activity. ChemBioChem 14:1049–1052. http://dx.doi.org/10.1002/cbic.201300207.

23. Heuer D, Brinkmann V, Meyer TF, Szczepek AJ. 2003. Expression and translocation of chlamydial protease during acute and persistent infection of the epithelial HEp-2 cells with Chlamydophila (Chlamydia) pneumoniae. Cell. Microbiol. 5:315–322. http://dx.doi.org/10.1046/j.1462-5822.2003.00278.x.

24. Belland RJ, Scidmore MA, Crane DD, Hogan DM, Whitmire W, McClarty G, Caldwell HD. 2001. Chlamydia trachomatis cytotoxicity associated with complete and partial cytotoxin genes. Proc. Natl. Acad. Sci. U. S. A. 98:13984–13989. http://dx.doi.org/10.1073/pnas.241377698.

25. Tipples G, McClarty G. 1993. The obligate intracellular bacterium Chlamydia trachomatis is auxotrophic for three of the four ribonucleoside triphosphates. Mol. Microbiol. 8:1105–1114. http://dx.doi.org/10.1111/j.1365-2958.1993.tb01655.x.

26. Adibhatla RM, Hatcher JF, Gusain A. 2012. Tricyclodecan-9-yl-xanthogenate (D609) mechanism of actions: a mini-review of literature. Neurochem. Res. 37:671–679. http://dx.doi.org/10.1007/s11064-011-0659-z.

27. Pütz U, Schwarzmann G. 1995. Golgi staining by two fluorescent ceramide analogues in cultured fibroblasts requires metabolism. Eur. J. Cell Biol. 68:113–121.

28. Matrosovich M, Matrosovich T, Garten W, Klenk H-D. 2006. New low-viscosity overlay medium for viral plaque assays. Virol. J. 3:63. http://dx.doi.org/10.1186/1743-422X-3-63.

29. Banks J, Eddie B, Sung M, Sugg N, Schachter J, Meyer KF. 1970. Plaque reduction technique for demonstrating neutralizing antibodies for Chlamydia. Infect. Immun. 2:443–447.

30. Hobson D, Stefanidis D, Rees E, Tait IA. 1982. Effects of chloramphenicol on Chlamydia trachomatis infection in neonatal conjunctivitis and in McCoy cell cultures. J. Hyg. 89:457–466. http://dx.doi.org/10.1017/S0022172400071023.

31. de Melo EJ, de Souza W. 1996. Pathway of C6-NBD-Ceramide on the host cell infected with Toxoplasma gondii. Cell Struct. Funct. 21:47–52. http://dx.doi.org/10.1247/csf.21.47.

32. Huitema K, van den Dikkenberg J, Brouwers JFHM, Holthuis JCM. 2004. Identification of a family of animal sphingomyelin synthases. EMBO J. 23:33–44. http://dx.doi.org/10.1038/sj.emboj.7600034.

33. Kuhle V, Abrahams GL, Hensel M. 2006. Intracellular Salmonella enterica redirect exocytic transport processes in a Salmonella pathogenicity island 2-dependent manner. Traffic 7:716–730. http://dx.doi.org/10.1111/j.1600-0854.2006.00422.x.

34. Lipsky NG, Pagano RE. 1985. A vital stain for the Golgi apparatus. Science 228:745–747. http://dx.doi.org/10.1126/science.2581316.

35. Hackstadt T, Scidmore MA, Rockey DD. 1995. Lipid metabolism in Chlamydia trachomatis-infected cells: directed trafficking of Golgi-derived sphingolipids to the chlamydial inclusion. Proc. Natl. Acad. Sci. U. S. A. 92:4877–4881. http://dx.doi.org/10.1073/pnas.92.11.4877.